

UNCLASSIFIED

Defense Technical Information Center
Compilation Part Notice

ADP013658

TITLE: An Effective Fourth Order Finite Volume Method for DNS/LES on Non-Uniform Grid

DISTRIBUTION: Approved for public release, distribution unlimited

This paper is part of the following report:

TITLE: DNS/LES Progress and Challenges. Proceedings of the Third AFOSR International Conference on DNS/LES

To order the complete compilation report, use: ADA412801

The component part is provided here to allow users access to individually authored sections of proceedings, annals, symposia, etc. However, the component should be considered within the context of the overall compilation report and not as a stand-alone technical report.

The following component part numbers comprise the compilation report:

ADP013620 thru ADP013707

UNCLASSIFIED

AN EFFECTIVE FOURTH ORDER FINITE VOLUME METHOD FOR DNS/LES ON NON-UNIFORM GRID

P. IANNELLI, F. M. DENARO, G. DE STEFANO

Dipartimento di Ingegneria Aerospaziale

Seconda Università di Napoli, Aversa, Italia

Abstract

This paper is concerned with the development of a fourth order Finite Volume scheme for the numerical solution of the incompressible Navier-Stokes equations on non-uniform grids. In fact, the use of non-uniform computational grids is inevitable in handling non-homogeneous flow computations, while numerical simulation of turbulent flows demand for higher order schemes. The effective high order accuracy is obtained by reformulating the momentum equation in terms of a fourth order deconvolved velocity field. Both a proper integration and flux reconstruction is implemented for the space discretization. A Fractional Time-Step method for the pressure-velocity de-coupling is adopted and a second order semi-implicit scheme is used for the time integration. Particular attention has been devoted in developing congruent time-accurate intermediate boundary conditions for the predictor step.

1. Introduction

Direct Numerical Simulations (DNS) as well as Large Eddy Simulation (LES) demand for accurate and efficient numerical schemes due to the wide range of length scales involved in a turbulent flow. In fact, low order methods show high numerical errors in the smallest resolved scales. As a matter of fact, for a long time, the numerical simulation of turbulent flows has been carried out by means of second order Finite Difference (FD) central scheme since, from the LES point of view, one performs an implicit application of the *top-hat* spatial filter. Moreover, LES on non-uniform grids were initially performed in a straightforward manner without taking into account for the existing commutation error, while only recently the correct equations for LES on non-uniform grids were analysed [1] and much more importance was given to the correlation between numerical errors and modelling ones (e.g.: [2]). More recently, conservative fourth order FD schemes were proposed over both staggered and co-located non-uniform grids (e.g.: [3]).

As it regards with the Finite Volume (FV) method, the integral form of the Navier-Stokes equations appears the most opportune by a physical point of view, allowing mass and momentum to be *a-priori* conserved. In this framework, an evolution equation for the volume-averaged field $\bar{\mathbf{v}}$ is solved, obtaining a second order approximation for the point-wise velocity \mathbf{v} , even by adopting higher-order

fluxes integration. Very recently, a fourth order FV compact scheme was proposed in [4], where a deconvolution technique was proposed in order to recover fourth-order accuracy from the volume averaged velocity field. Actually, such procedure was applied only in a post-processing step while the solved variable remains the second order averaged one.

On the contrary, in this paper, we follow the approach already introduced in the framework of the so-called Implicit Structural Models [5, 6]. In that approach, a modified integral equation, governing the evolution of an effective fourth-order variable, is obtained by means of a de-convolution procedure applied on the original FV equations. Following such guidelines, the development of a high order FV scheme on non-uniform grid is illustrated in the framework of the Fractional Time-Step (FTS) method for pressure-velocity de-coupling. The spatial discretization is performed according to the Simpson integration rule while proper Lagrange interpolation is used for the fluxes reconstruction. The time integration is performed by means of the semi-implicit Adams-Bashforth/Crank-Nicolson (AB/CN) scheme. Finally, time-accurate boundary conditions to be associate to the predictor equation were developed in a manner consistent with the adopted time integration. The proposed method has been validated in the numerical simulation of both the two-dimensional Taylor decaying vortex solution and a time evolving mixing layer.

2. Deconvolved Navier Stokes Equations On Non-Uniform Grids

Consider the Navier-Stokes equations for incompressible isothermal flows in a bounded domain V , written in integral non-dimensional form over a Finite Volume (FV) $\Omega(\mathbf{x}) \subseteq V$, centred in \mathbf{x} , whose boundary is denoted by $\partial\Omega(\mathbf{x})$:

$$\int_{\partial\Omega(\mathbf{x})} \mathbf{n} \cdot \mathbf{v} \, dS = 0 \quad , \quad (1)$$

$$\frac{\partial \bar{\mathbf{v}}}{\partial t} + \frac{1}{|\Omega(\mathbf{x})|} \int_{\partial\Omega(\mathbf{x})} \mathbf{n} \cdot \mathbf{F} \, dS = \mathbf{0} \quad (2)$$

being $\bar{\mathbf{v}}$ the local volume averaged velocity, $|\Omega(\mathbf{x})|$ the measure of the FV, \mathbf{n} the local unit vector outward to the boundary $\partial\Omega$ and \mathbf{F} the momentum flux tensor, expressed as $\mathbf{v}\mathbf{v} + \mathbf{I}p - \underline{\nabla}\mathbf{v}/\text{Re}$. A proper initial field \mathbf{v}_0 and boundary conditions \mathbf{v}_b on ∂V must be associated to the system (1)-(2).

Following the formulation proposed in [5], an m -th order Taylor expansion for \mathbf{v} around the FV centre \mathbf{x} is performed, being m an even integer. Owing to the cell symmetry, one gets (for sake of brevity, time dependence is omitted):

$$\bar{\mathbf{v}}(\mathbf{x}) = (I_{\mathbf{x}} - R_{\mathbf{x}}^{(m)})\mathbf{v} + O(h^{m+2}) \equiv G_{\mathbf{x}}^{(m)}\mathbf{v} + O(h^{m+2}) \quad (3)$$

being h a linear extension of the FV, e.g. $h=|\Omega(\mathbf{x})|^{1/3}$. The differential operator

$R_{\mathbf{x}}^{(m)} \equiv -\sum_{l=1}^m \frac{1}{l!} \sum_{i_1+i_2+i_3=l} C_{i_1,i_2,i_3}(\mathbf{x}) D_{\mathbf{x}}^{(i_1,i_2,i_3)}$ was introduced, being $D_{\mathbf{x}}^{(i_1,i_2,i_3)} = \partial_{x_1}^{i_1} \partial_{x_2}^{i_2} \partial_{x_3}^{i_3}$ the

l -th order three-dimensional derivative in a Cartesian reference system and

$$C_{i_1, i_2, i_3}(\mathbf{x}) = \frac{1}{|\Omega(\mathbf{x})|} \prod_{k=1}^3 \int_{\Omega(\mathbf{x})} (x'_k - x_k)^{i_k} d\mathbf{x}'$$

the coefficients of the moments of the

Taylor expansion terms. By truncating and inverting Eq.(3), one obtains the m -th order de-convolved velocity $\tilde{\mathbf{v}}(\mathbf{x}) \equiv [G_{\mathbf{x}}^{(m)}]^{-1} \bar{\mathbf{v}}$, whose properties in both physical and Fourier space were analysed in [5]. If the inverse operator $[G_{\mathbf{x}}^{(m)}]^{-1}$ is applied on Eq.(2), one gets an evolution equation for the de-filtered field $\tilde{\mathbf{v}}$, but commutation terms appear for non-uniform grids. Herein, in order to avoid the explicit computation of such terms, the LHS of Eq.(2) is simply re-written, so that:

$$G_{\mathbf{x}}^{(m)} \frac{\partial \tilde{\mathbf{v}}}{\partial t} = \mathbf{I}_{conv} + \mathbf{I}_{diff} + \mathbf{I}_{press} \tag{4}$$

with

$$\mathbf{I}_{press} = -\frac{1}{|\Omega(\mathbf{x})|} \int_{\partial\Omega(\mathbf{x})} dS \mathbf{n} \cdot \mathbf{I}p \quad ; \quad \mathbf{I}_{conv} = -\frac{1}{|\Omega(\mathbf{x})|} \int_{\partial\Omega(\mathbf{x})} dS \mathbf{n} \cdot \mathbf{v}\mathbf{v} \quad ; \tag{5}$$

$$\mathbf{I}_{diff} = \frac{1}{\text{Re} |\Omega(\mathbf{x})|} \int_{\partial\Omega(\mathbf{x})} dS \mathbf{n} \cdot \underline{\nabla} \mathbf{v} \equiv \frac{1}{\text{Re}} D\mathbf{v} \quad ; \quad D \equiv \frac{1}{|\Omega(\mathbf{x})|} \int_{\partial\Omega(\mathbf{x})} dS \mathbf{n} \cdot \underline{\nabla}(\bullet)$$

As a matter of fact, from the LES point of view, Eq. (4) should be supplied with a suitable Sub-Grid Scales (SGS) model, in order to express the RHS in terms of the resolved variable $\tilde{\mathbf{v}}$. However, in this paper, we just consider $\mathbf{F}(\mathbf{v}) \approx \mathbf{F}(\tilde{\mathbf{v}})$ without addressing this issue. In the framework of Implicit Structural Models [6], this can be interpreted as an LES approach for the *top-hat* filtered variable, supplied by a sort of generalized scale similarity SGS model. Finally, the de-convolution order is fixed to $m=2$ ($G_2 \equiv G_{\mathbf{x}}^{(2)}$) in order to get $\tilde{\mathbf{v}}$ representing an effective fourth-order approximation to the point-wise velocity field.

3. A Fourth Order Deconvolution-based Scheme on Non-Uniform Grids

In this section, a fourth order FV method is developed for 2-D flows simulation on Cartesian non-uniform grids. The de-coupling between the velocity and the pressure gradient is performed according to the FTS method [7], while the semi-implicit Adams-Bashforth/Crank-Nicolson second order scheme is adopted for the time integration. Furthermore, let us assume the computational domain $V = [0, L_1] \times [0, L_2]$. Owing to its computational simplicity, a co-located arrangement of the variables was adopted, hence the flux vectors defined onto the face-nodes must be approximated in terms of the balanced variables in the FV centre nodes.

3.1. Two-Dimensional Grid Definition

The grid points (see Fig.1) are uniformly distributed in x -direction (supposed to

be a stream-wise direction), i.e., $x_i = (i-1)h_1 + h_1/2$, with $h_1=L_1/N_1$ the step size, $i=1, \dots, N_1$, being N_1 the number of FVs in x - direction. The y -direction (supposed to be a normal wall one) has non-uniform grid spacing obtained by means of an 1-D mapping $y=Y(\zeta)$, being ζ the independent variable in the computational domain. This latter is uniformly discretized by a step size $H=L_2/N_2$, being N_2 the number of FVs in y -direction. Furthermore, for each FV the face co-ordinates $y_j^- = Y(\zeta_j)$ and $y_j^+ = Y(\zeta_{j+1})$, are defined for $j=1, \dots, N_2$ and thus, the FV grid node results $y_j = (y_j^- + y_j^+)/2$, being $y_j^- = y_{j-1}^+$ for grid construction. The mesh size in y -direction is defined as $h_2(j) = y_j^+ - y_j^- = Y(\zeta_{j+1}) - Y(\zeta_j)$ having assumed a smooth mapping ($h_2/H = O(1)$) so that, the FV definition is $\Omega_{ij} \equiv [x_i - h_1/2; x_i + h_1/2] \times [y_j - h_2(j)/2; y_j + h_2(j)/2]$. It is noteworthy that one can simply express the face co-ordinates as $x_i^\pm = x_i \pm h_1/2$, $y_j^\pm = y_j \pm h_2(j)/2$.

3.2. The FTS Procedure and The Discrete Time Integration

In Eqs.(1) and (4) the diffusive terms along the y -direction are integrated in time by means of the Crank-Nicolson scheme, while the Adams-Bashforth one is adopted for all the other terms. In the present FTS method (*pressure-free projection method*), first an equation for a non-solenoidal vector \mathbf{v}^* is obtained by integrating Eq.(4) and eliminating the pressure term:

$$\left(G_2 - \frac{\Delta t}{2\text{Re}} D_y \right) \mathbf{v}^* = \left[G_2 + \frac{\Delta t}{2\text{Re}} (D_y + 3D_x) \right] \mathbf{v}^n + \frac{\Delta t}{2} \left(3\mathbf{I}_{conv}^n - \frac{1}{\text{Re}} D_x \mathbf{v}^{n-1} - \mathbf{I}_{conv}^{n-1} \right) \quad (6)$$

in V

$$\mathbf{v}^* = \mathbf{v}_b^*$$

on ∂V

$$D_x \equiv \frac{1}{|\Omega(\mathbf{x})|} \int_{y^-}^{y^+} d\eta \left(\frac{\partial}{\partial \xi} \Big|_{x^+} - \frac{\partial}{\partial \xi} \Big|_{x^-} \right) ; \quad D_y \equiv \frac{1}{|\Omega(\mathbf{x})|} \int_{x^-}^{x^+} d\xi \left(\frac{\partial}{\partial \eta} \Big|_{y^+} - \frac{\partial}{\partial \eta} \Big|_{y^-} \right)$$

In the previous relations, the operator D was split as $D = D_x + D_y$, along the Cartesian directions, being x^\pm and y^\pm the face co-ordinates of Ω . Observe that the de-convolution procedure does not increase the computational cost since a semi-implicit procedure has been adopted for the time integration. Therefore, the LHS will simultaneously take into account for both deconvolution and time integration

The predicted velocity field \mathbf{v}^* must be corrected by means of a pure gradient field according to:

$$\mathbf{v}^{n+1} \equiv \mathbf{v}^* - \underline{\nabla} \phi \quad (7)$$

Therefore, once the vector field \mathbf{v}^* was computed, the continuity constraint is enforced at the new time level t^{n+1} by means of the *projection* step:

$$D\phi = \frac{1}{|\Omega(\mathbf{x})|} \int_{\partial\Omega(\mathbf{x})} \mathbf{n} \cdot \mathbf{v}^* dS \quad ; \quad \frac{\partial\phi}{\partial n} = \mathbf{n} \cdot (\mathbf{v}^* - \mathbf{v}_b^{n+1}) \text{ on } \partial V \quad (8)$$

associated to the proper normal boundary conditions.

3.3. Fourth Order Spatial Discretization

The achievement of a real fourth order space accuracy is obtained by means of the Simpson integral discretization along with explicit Lagrangian interpolation for the fluxes discretization. Although, at the same accuracy, a Lagrangian polynomial involves a wider stencil than a Hermitian interpolation (as recently proposed in [4]), the former approach remains simply applicable in the non-

uniform direction. The operator $G_2 = I_x + \frac{h_1^2}{24} \frac{\partial^2}{\partial \xi^2} \Big|_{x'=x} + \frac{h_2^2(y)}{24} \frac{\partial^2}{\partial \eta^2} \Big|_{x'=x}$ is

discretized to fourth order accuracy by considering second order central difference formulas for the spatial derivatives. Having deconvolved the velocity field to fourth order accuracy, the integral fluxes in Eqs.(6) and (8) are congruently discretized by means of the Simpson formula. In such a way, one has, as an example, for the net flux along x -direction:

$$\int_{y_j^-}^{y_j^+} [f(x_i^+, \eta) - f(x_i^-, \eta)] d\eta = \frac{h_2}{6} (f_{i,j^+} + 4f_{i,j} + f_{i,j^-}) \Big|_{i^-}^{i^+} - \frac{h_1 h_2^5}{2880} \frac{\partial^5 f}{\partial \xi \partial \eta^4} \Big|_{i,j} + \dots \quad (9)$$

wherein, the face-node unknowns (see Fig.1) are expressed in terms of the grid nodes values. A high-order Lagrangian interpolation procedure is adopted by factorising the function along each direction and approximating both the factors by means of two third degree polynomials, i.e.: $f(x, y) \cong \hat{f}(x, y) = L_1(x)L_2(y)$. This way, one obtains a global 25 grid-nodes computational molecule.

3.4. Boundary Conditions

The original system (1), (4) was de-coupled in the separate prediction (6) and projection (8) equations. The solution of this latter, together with Eq. (7), allows the intermediate velocity \mathbf{v}^* to be corrected by imposing the exact normal velocity component $\mathbf{n} \cdot \mathbf{v}_b^{n+1}$ on ∂V . Since the projection can not correct the tangential velocity component, this latter must be congruently assigned for solving Eq.(6). In this paper we propose a procedure for assigning time accurate boundary conditions. In fact, by taking the limit of Eq.(6) for vanishing grid spacing ($G_2 \rightarrow I$ for $h \rightarrow 0$) and projecting it along the direction tangential to the boundary, one gets:

$$\left(v_i^* - \frac{\Delta t}{2\text{Re}} \frac{\partial^2 v_i^*}{\partial y^2} \right)_{\partial V} = \left(v_i^n + \frac{\Delta t}{2\text{Re}} \frac{\partial^2 v_i^n}{\partial y^2} \right)_{\partial V} + \frac{\Delta t}{2} \mathbf{t} \cdot \left\{ \nabla \cdot [(3\mathbf{v}\mathbf{v})^n - (\mathbf{v}\mathbf{v})^{n-1}] - \frac{1}{\text{Re}} \left(3 \frac{\partial^2 \mathbf{v}^n}{\partial x^2} - \frac{\partial^2 \mathbf{v}^{n-1}}{\partial x^2} \right) \right\}_{\partial V} \quad (10)$$

When properly spatially discretized, Eq.(10) provides the correct second order time accurate solution on the frontier, as illustrated in the next section.

4. Numerical Results

The adopted test case is the classical 2-D Taylor decaying vortex solution at $Re=1$. The error estimations are performed in the computational domain $V=[-\pi, \pi] \times [-\pi, \pi]$, by taking the L_∞ norm of the difference between the x -component of the exact and numerical velocity field. In a first test, for bi-periodical boundary conditions, the effect of the de-averaging procedure was studied, having used the fourth-order flux integration (9). The resulting errors, computed after 100 time steps ($\Delta t=10^{-4}$), are shown in Fig.2 versus the normalised grid size in a double logarithmic scale, for both uniform and non-uniform grids. It can be noted that only in the presence of the de-averaging procedure ($m=2$) an effective fourth order accuracy is reached in computing unsteady solutions. The space accuracy is also checked for Dirichelet boundary conditions in the y -direction, as illustrated in Fig.3 on both uniform and non-uniform grids. Moreover, the correctness of the proposed boundary conditions (10) is analysed from the results in Fig.4, where the time accuracy tests is reported. A single time integration was conducted in order to avoid stability problems when working with high time steps. The errors are reported versus the used time step, showing a third order slope according to the fact we are evaluating the direct error on a single time step, that corresponds to a second-order local truncation error.

Finally, the procedure was tested for a time evolving mixing layer. The initial configuration is the same adopted in [9], i.e. a hyperbolic tangential velocity profile $u(y) = u_\infty \tanh 2y/\delta_1$ (being $2\delta_1$ the initial vorticity thickness) submitted to a white noise perturbation plus a deterministic sine perturbation at $k_t=(2\pi/\lambda_a)$ with $\lambda_a=7\delta_1$. Kelvin-Helmholtz instabilities lead to the development of vortices which in a later stage roll-up and merge. This is a good example for the tendency of 2D turbulence to transfer energy from small to large scales thus requiring an accurate numerical simulation. The preliminary results of this study are reported in Figs 5 for a 128^2 computational grid on a domain $V=[0, 4\lambda_a] \times [-2\lambda_a, 2\lambda_a]$ at $Re = u_\infty \delta_1 / \nu = 250$ showing the salient features of backscatter transfer energy and the appearance of a k^{-4} range according to the LES performed in [9].

References

1. S. Ghosal, P.Moin, The basic equations for the large eddy simulation of turbulence flows in complex geometry *J. Comp. Phys.*, 118, 1995.
2. A. G. Kravchenko, P. Moin, On the effect of numerical errors in Large Eddy Simulations of turbulent Flows. *J. Comp. Phys.*, 131, 1997.
3. Y. Morinishi, T.S. Lund, O. V. Vasilyev, P. Moin, Fully Conservative Higher Order Finite Difference Schemes for Incompressible Flow. *J. Comp. Phys.*, 143, 90-124, 1998.

4. J. M. C. Pereira, M. H. Kobayashi, J. C. F. Pereira, A fourth order accurate finite volume compact method for the incompressible Navier-Stokes solutions, *J. Comp. Physics*, in press, 2001.
5. G. De Stefano, F.M. Denaro, G. Riccardi, High order filtering for control volume flow simulations, *Int. J. Num. Methods in Fluids*, 37, 2001.
6. P. Sagaut, Large Eddy Simulation for incompressible flows. An introduction. (pp.198-200), Springer, 2001.
7. A. J. Chorin, Numerical Solution of the Navier-Stokes Equations, *Math. Comp.*, 22, 745-762, 1968.
8. J. Kim, P. Moin, Application of A Fractional-Step Method to Incompressible Navier-Stokes Equations, *J. Comp. Phys.*, 59, 308-323, 1985.
9. M. Lesieur, C. Staquet, P. Le Roy, P. Comte, The mixing layer and its coherence examined from the point of view of two-dimensional turbulence, *J. Fluid Mech.*, 192, 1986.

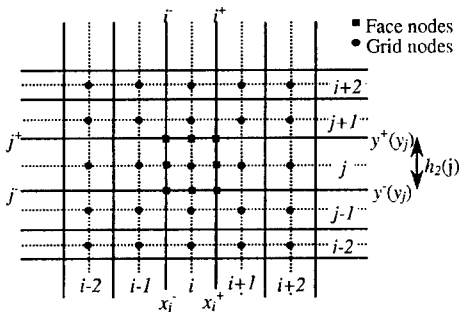


Figure 1: description of the adopted 2-D grid, non-uniform in the y- direction. For each j-th finite volume, the vertical flux section is centred with respect to the node j i.e., $y^\pm(y_j) = y_j \pm h_2(j)/2$. The unknown variables u, v, p are co-located on the grid nodes (●).

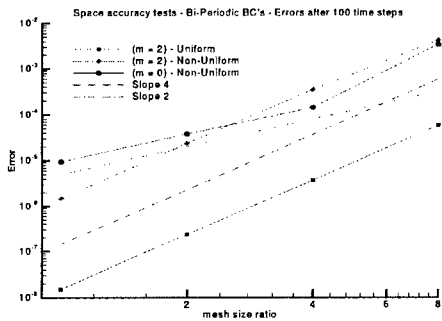


Figure 2: Space accuracy tests with Bi-periodic boundary conditions applied. Effects of the de-averaging procedure on the accuracy. Errors computed after 100 time steps on both uniform and non-uniform grids.

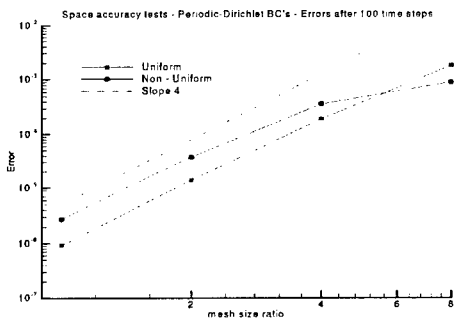


Figure 3: Space accuracy tests with Periodic-Dirichlet boundary conditions applied. Errors computed after 100 time steps on both uniform and non-uniform grids.

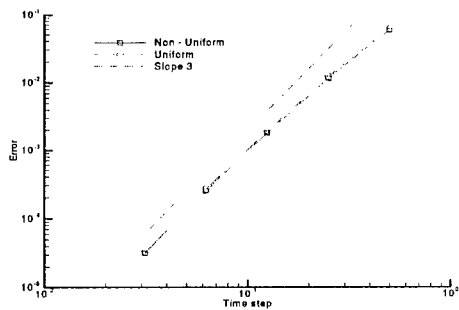


Figure 4: Time accuracy tests. Errors computed after one time steps on both uniform and non-uniform grids of 60^2 CV's.

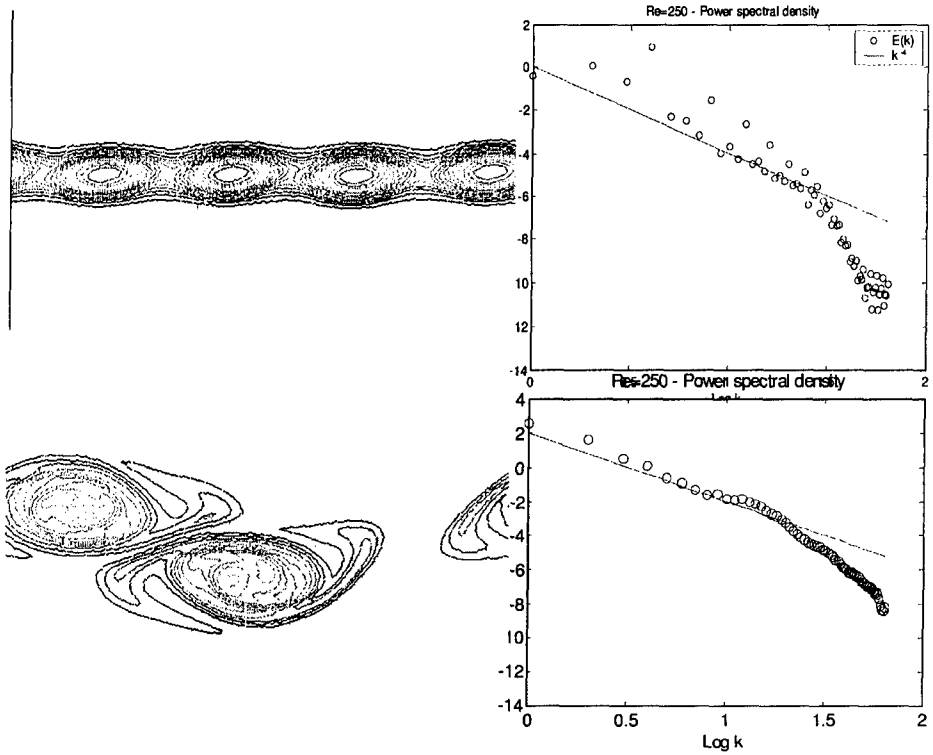


Figure 5: Time evolving mixing layer; isovorticity contours are on the left column while the one-dimensional energy spectra are on the right for $t = 35\delta_1 / u_\infty$ and $t = 65\delta_1 / u_\infty$.